CARDIAC ASSIST DEVICE DESIGN AND MATERIAL SELECTION: A REVIEW AND FINITE VOLUME STUDY

Zuzanna Zając[1*], Magdalena Kopernik[2], Justyna Więcek-Chmielarz[1], Karolina Szawiraacz[1], Przemysław Kurtyka[1,3], Marcin Surmiak[4,5], Mirjam Spuller[6,7], Jürgen M. Lackner[6], Roman Major[1*]

[1] Institute of Metallurgy and Materials Science Polish Academy of Sciences, 30-059 Kraków, Poland
[2] AGH University of Krakow, 30-059 Kraków, Poland
[3] Institute of Heart Prosthesis, Foundation of Cardiac Surgery Development, 41-800 Zabrze, Poland
[4] 2nd Department of Internal Medicine, Faculty of Medicine, Jagiellonian University Medical College, 30-688 Kraków, Poland
[5] Center for the Development of Therapies for Civilization and Age-Related Diseases, Jagiellonian University Medical College, 30-688 Kraków, Poland
[6] Joanneum Research Forschungsgesellschaft mbH, Materials – Institute for Sensors, Photonics and Manufacturing Technologies, 8712 Niklasdorf, Austria
[7] Doctoral School of Chemistry, Graz University of Technology, 8010 Graz, Austria
* e-mail: zajac.z@imim.pl, major.r@imim.pl

Abstract

Cardiovascular diseases (CVDs) remain the leading cause of mortality worldwide and represent a major public health challenge. Mechanical circulatory support (MCS) devices, particularly blood pumps used in ventricular assist systems, have become an important therapeutic option for patients with advanced heart failure. Despite significant technological progress, the long-term performance of these devices remains limited by hemocompatibility issues, including hemolysis, thrombosis, and platelet activation. These complications arise from the complex interactions between blood flow dynamics, device geometry, and the properties of blood-contacting biomaterials. This work presents an interdisciplinary analysis combining a review of biomaterials used in blood-contacting devices with a numerical investigation of hemodynamic conditions in a rotary blood pump. To investigate the relationship between flow conditions and potential blood damage, computational fluid dynamics simulations based on the finite volume method (FVM) were performed. The analysis included pressure, velocity, wall shear stress, and power distributions using the Casson non-Newtonian blood model and the k-ω SST turbulence model for a 3D two-blade rotor configuration. The results indicate that the highest values of pressure, velocity, and wall shear stress occur near blade edges, where flow acceleration and turbulence intensify, potentially increasing the risk of hemolysis and platelet activation. These findings highlight the importance of integrating optimized rotor geometry, advanced biomaterial surfaces, and contact-free bearing technologies, such as magnetic levitation, in the design of next-generation blood pumps.

Keywords: *blood pumps; hemocompatibility; blood-contacting biomaterials; computational fluid dynamics (CFD); finite volume method (FVM); wall shear stress*

List of Abbreviations

a-C:H – Hydrogenated Amorphous Carbon
AM – Additive Manufacturing
BA – Bees Algorithm
CFD – Computational Fluid Dynamics
Co-Cr-Mo – Cobalt-Chromium-Molybdenum
CVD – Cardiovascular Disease
DLC – Diamond-Like Carbon
FDA – Food and Drug Administration
FVM – Finite Volume Method
GAs – Genetic Algorithms
LES – Large Eddy Simulation
LVAD – Left Ventricular Assist Device
MCS – Mechanical Circulatory Support
PCE – Polynomial Chaos Expansions
PCL – Polycaprolactone
PCU – Poly(carbonate-urea)urethane
PET – Polyethylene Terephthalate
PEU – Poly(ether urethane)
PHAs – Polyhydroxyalkanoates
PLA – Polylactic Acid
PTFE – Polytetrafluoroethylene
PU – Polyurethane
RANS – Reynolds-Averaged Navier–Stokes
SBES – Stress-Blended Eddy Simulation
SS – Stainless Steel
SST k-ω – Shear Stress Transport k–omega
Ti – Titanium
UQ – Uncertainty Quantification
VAD – Ventricular Assist Devices

Introduction

Cardiovascular diseases (CVDs) remain the leading cause of mortality worldwide and represent a major public health challenge. In the European Union, CVDs account for more than 30% of all annual deaths and affect over 60 million individuals [1, 2]. According to the World Health Organization, CVDs encompass a broad spectrum of disorders affecting the heart and vascular system, including coronary artery disease, cerebrovascular disease, peripheral arterial disease, rheumatic and congenital heart conditions, as well as venous thromboembolism such as deep vein thrombosis and pulmonary embolism [3]. These conditions involve both structural abnormalities and functional impairments of the circulatory system and impose a significant clinical and socioeconomic burden on healthcare systems.

The development and progression of cardiovascular diseases are strongly influenced by modifiable lifestyle and environmental factors. Among the most significant contributors are a sedentary lifestyle, tobacco use – including both conventional and electronic cigarettes – excessive alcohol consumption, unhealthy diets rich in salt and saturated fats, chronic stress, and obesity [4, 5]. Numerous epidemiological studies have demonstrated that lifestyle interventions can significantly reduce the incidence of cardiovascular diseases and their associated risk factors. In particular, dietary patterns characterized by increased consumption of whole grains, fruits, and vegetables have been associated with

[Engineering of Biomaterials 174 (2026) 14]

doi:10.34821/eng.biomat.174.2026.14

Submitted: 2026-06-12, Accepted: 2026-07-21, Published: 2026-07-27

improved cardiovascular health and a lower prevalence of hypertension, dyslipidemia, and metabolic disorders [6, 7].

Despite considerable progress in pharmacological treatment and preventive strategies, many cardiovascular diseases progress to advanced stages such as severe heart failure. In such cases, conventional medical therapy may no longer provide sufficient circulatory support, making the use of mechanical circulatory support (MCS) systems necessary. Although heart transplantation remains the gold standard for the treatment of end-stage heart failure, its widespread clinical application is limited by the persistent shortage of suitable donor organs and strict eligibility criteria [8-10]. Consequently, mechanical heart support systems have emerged as an essential therapeutic alternative, serving as a bridge to transplantation, a bridge to recovery, or as destination therapy for patients who are not eligible for transplantation. Among MCS technologies, ventricular assist devices (VADs) have undergone significant technological evolution, transitioning from large pulsatile pumps to compact continuous-flow systems characterized by improved durability, efficiency, and reduced mechanical complexity [11]. In recent years, particular attention has been directed toward the development of highly miniaturized heart assist pumps. These next-generation devices are designed to enable minimally invasive implantation and to expand therapeutic options for patient populations that were previously underserved, including pediatric patients and individuals with smaller body sizes. Advances in microengineering, rotor design, and biomaterials have facilitated the development of ultra-compact pumps capable of being implanted via vascular access rather than through highly invasive surgical procedures [12, 13]. Such miniaturized ventricular assist devices have the potential to significantly reduce surgical trauma, improve patient recovery, and enable earlier intervention in the progression of heart failure.

However, despite substantial progress in device design, long-term performance of heart assist pumps remains challenged by complications such as thrombosis, hemolysis, and device-induced blood damage. These adverse events are strongly influenced by the interaction between blood flow patterns, shear stresses generated by the rotor, and the physicochemical properties of blood-contacting biomaterials [14]. Therefore, optimizing rotor geometry, hemodynamic performance, and surface properties is essential to improve hemocompatibility and overall device reliability.

In this context, the present work aims to provide a review of heart support systems with particular emphasis on rotor design and biomaterials used in ventricular assist devices, including emerging miniaturized pump technologies. Furthermore, the study investigates their performance and hemodynamic characteristics using finite volume method analysis to better understand the relationship between device geometry, flow dynamics, and potential mechanisms of blood damage.

Mechanical Circulatory Support

Since the first successful implantation of a left ventricular assist device (LVAD) in humans, performed by Michael DeBakey in 1963, followed by the first artificial heart implantation by Denton Cooley in 1969, continuous efforts have been undertaken within the academic and clinical communities to advance the design and performance of mechanical circulatory support systems [15]. Several strategies of mechanical circulatory support (MCS) have been established to address different clinical scenarios, including bridge to decision, bridge to recovery, bridge to transplant, and destination therapy, with each approach selected according to the patient's specific condition and treatment goals [16-18]. A wide range of cardiac assist devices is currently available on the market, some of which are summarized in TABLE 1. These systems are broadly classified into pulsatile, axial-flow, and centrifugal-flow pumps.

Pulsatile Blood Pumps

Pulsatile pumps were the first type of mechanical circulatory support devices developed to assist or replace the pumping function of the failing heart [28]. These devices are designed to mimic the physiological cardiac cycle by generating a pulsatile blood flow, which resembles the natural pattern of systole and diastole observed in the human cardiovascular system. An example of a pulsatile pump is shown in FIG. 1.

FIG. 1. Example of a pulsatile mechanical circulatory support pump (source: Foundation of Cardiac Surgery Development in Zabrze [29])

The main difference between pulsatile and centrifugal pumps lies in the nature of the generated blood flow. Pulsatile pumps reproduce the physiological rhythm of the heart rather than providing a continuous flow. This flow pattern is considered beneficial for maintaining more natural hemodynamic conditions and may reduce damage to blood components. However, pulsatile pumps are typically relatively large and mechanically complex devices. Their operation is also associated with increased noise compared to other types of circulatory support systems, which may negatively affect patient comfort. Consequently, despite their physiological flow characteristics, the large size and mechanical complexity of pulsatile pumps have led to their gradual replacement in modern clinical practice by smaller continuous-flow devices, such as centrifugal and axial flow pumps [30].

Centrifugal Blood Pump

Centrifugal blood pumps typically consist of a disk-shaped housing containing a rotating impeller. Blood enters the pump through the inlet and flows toward the central region of the impeller. The rotating impeller imparts kinetic energy to the blood, generating a centrifugal force that drives the flow radially outward toward the pump outlet and subsequently into the aorta [31]. Key parameters in the design of such devices include the dimensions of the inlet and outlet ports, the overall pump size, and the geometry of the impeller. Particular attention is devoted to impeller design, including blade angle, curvature, and thickness, as these features strongly influence hemodynamic performance, hemocompatibility, and overall device efficiency [17, 32].

Centrifugal blood pumps are relatively compact devices, which is a highly desirable feature from the perspective of patient comfort [32]. They also operate more quietly than pulsatile pumps. Another advantage is the relatively simple implantation procedure, which facilitates their broader clinical application. In addition, centrifugal pumps are generally less expensive than other types of mechanical circulatory support devices [33].

TABLE 1. Comparison of heart support systems, including rotor type and maximum flow rate

Pump model	Manufacturer	Rotor type	Maximum Flow rate [L/min]	Additional information	References
CentriMag	Abbott, Thoratec, Pleasanton, CA, Unitet States of America)	Magnetically levitated centrifugal pump	10	Approved for short-term use (up to 30 days); Supports LVAD, RVAD, or BiVAD	[23]
Deltastream DP3 diagonal rotary pump	Medos Medizintechnik AG, Stolberg, Germany	Rotary blood pump with combined characteristics of an axial and a radial design	8	Pediatric patients with end-stage congenital heart disease, cardiomyopathies, or fulminant myocarditis; Patients with heart failure awaiting recovery; Patients with difficulty weaning from cardiopulmonary bypass; Patients awaiting heart transplantation	[24]
Bio-pump BPX-80	Medtronic, Inc., Minneapolis, MN, Unitet States of America	Mechanical bearing centrifugal pump	10	Provides extracorporeal circulatory support for periods suitable for cardiopulmonary bypass (up to 6 hours); Indicated for short-term extracorporeal support	[25]
Impella 5.5®	Abiomed, Berlin, Germany	Axial flow pump	5	Longer-term mechanical support (up to ~29 days); Enables patient ambulation during therapy; Integrated SmartAssist real-time monitoring system; Approved support duration: up to 14 days (FDA, USA); up to 30 days (CE, Europe)	[19, 20, 22, 27]
HeartMate 3™ Left Ventricular Assist Device (LVAD)	Abbott, Thoratec, Pleasanton, CA, United States of America	Fully levitated, self-centering rotor	10	Bridge to transplantation: short-term support for patients awaiting heart transplantation; Destination therapy: long-term or permanent support for patients ineligible for transplantation	[21, 26]
HeartWare™ HVAD™	Medtronic, Inc., Minneapolis, MN, United States	Radial-flow pump with magneto-hydrodynamic impeller suspension	10	Indication: end-stage heart failure	[16]

Axial Flow Pump

Axial flow pumps are typically tubular devices that contain a screw-shaped impeller positioned along the central axis of the pump. During rotation, the impeller generates a continuous axial flow, propelling blood through the device from the left ventricle to the ascending aorta [32]. The main difference between axial and centrifugal pumps lies in the direction of blood flow within the device. In axial pumps, the flow direction remains largely unchanged as blood moves along the axis of the impeller, whereas centrifugal pumps redirect the flow radially outward.

Axial flow pumps are generally smaller than centrifugal pumps. However, due to their compact design, they typically operate at higher rotational speeds to achieve the desired flow rates [34]. Their small size also facilitates a relatively quick and straightforward implantation procedure. Moreover, axial pumps usually require lower power consumption compared to centrifugal devices, which allows for the use of smaller external power units and contributes to improved patient comfort [35].

Challenges and Complications Associated with Cardiac Assist Devices

Despite considerable progress in the development of cardiac assist pumps, multiple challenges remain, including clinical complications as well as issues related to material properties and hemodynamics. Among clinical complications, infections remain one of the most common adverse events, affecting approximately 18% to 59% of patients [15, 36] and representing a major challenge in long-term therapy. Another serious complication is stroke, which is one of the leading causes of disability and mortality in patients supported with cardiac assist devices [37].

Another important complication is bleeding, the risk of which is increased by the use of anticoagulant therapy, commonly required in patients supported with mechanical circulatory devices [15]. The need for anticoagulation arises from the exposure of blood to elevated shear stresses within the pump, which can lead to the degradation of von Willebrand factor [15]. This glycoprotein plays a crucial role in hemostasis, as it promotes platelet adhesion to

thrombogenic surfaces as well as platelet-to-platelet cohesion during thrombus formation [38]. Its degradation therefore results in impaired platelet function and contributes to an increased risk of bleeding [15].

In contrast to bleeding complications, another significant adverse event is thromboembolism, which may occur both as a result of thrombus formation on the pump material and within the patient's circulatory system [17]. Such events are extremely dangerous and pose a serious risk to both patient health and survival. A dislodged thrombus traveling through the bloodstream can lead to severe complications, including stroke [17, 39]. Thrombus formation within the pump itself can also markedly impair device performance by disrupting blood flow. For this reason, anticoagulant therapy is routinely administered.

Role of Biomaterials

Material requirements for blood-contacting devices

Materials intended for use in cardiac assist pumps, as blood-contacting biomaterials operating under significant shear stress conditions, must meet a range of stringent requirements. A key property of materials intended for blood-contacting applications is hemocompatibility, which refers to the manner in which a foreign material interacts with blood while inducing minimal adverse effects [40]. A material is considered hemocompatible when it does not significantly disrupt blood components, particularly with respect to hemolysis [40]. Shear stress is one of the primary factors contributing to the occurrence of hemolysis [41]. Under physiological conditions, shear stress levels within blood vessels remain relatively low and tightly regulated. However, in cardiac assist devices, particularly in rotary pumps, shear stress can reach significantly higher values due to rapid flow acceleration and complex flow patterns.

Typical wall shear stress values in the human vasculature vary depending on vessel type and physiological conditions. In large arteries, shear stress is generally reported in the range of approximately 1.4–3.6 Pa, while in arterioles it may reach higher values of about 2.0–7.2 Pa. In contrast, venous shear stresses are significantly lower, typically between 0.07 and 0.9 Pa. Under pathological conditions, such as in stenotic vessels, shear stress can increase substantially, reaching values on the order of 3.6 up to 45 Pa [42].

In comparison, mechanical circulatory support devices are associated with markedly elevated shear stress levels. Rotary centrifugal pumps typically generate stresses in the range of approximately 50–320 Pa, whereas rotary axial devices may produce even higher values, exceeding 200 Pa in some cases. Positive displacement pumps generally operate at intermediate levels, often reported between about 10 and 50 Pa. These differences highlight the significantly more extreme hemodynamic environment present in blood-contacting medical devices compared to physiological conditions [42].

Hemolysis results in impaired red blood cell function, rendering them unable to effectively transport oxygen, which constitutes a serious and potentially life-threatening condition [41]. In general, hemocompatibility is assumed when the level of hemolysis remains below 5% [40]. In addition to hemolysis, hemocompatibility is also associated with reduced platelet activation, thrombosis, and inflammatory responses.

These materials must exhibit high biocompatibility, which, according to Ratner, can be defined as "the ability of a material to locally trigger and guide non-fibrotic wound healing, reconstruction, and tissue integration" [43]. Ratner also introduced the concept of biotolerability, defined as "the ability of a material to reside in the body for long periods of time with only low degrees of inflammatory reaction", which is crucial for ensuring the safety of biomaterials [43]. In addition, such materials must possess appropriate mechanical properties and demonstrate resistance to long-term operation under repeated cyclic loading.

Material Classes for blood-contacting devices

Cardiac assist devices and their components are manufactured from a range of materials, including metals and their alloys, ceramics, polymers, as well as animal-derived tissues [32]. Material selection depends on the specific application, and different material classes are often combined to achieve the desired functional properties. A summary of the major material classes used in cardiac assist systems is presented in TABLE 2.

Among these material classes, metals - particularly titanium and its alloys - play a critical role in the construction of cardiac assist devices. Titanium and its alloys are widely used in biomedical engineering across various applications, including the fabrication of cardiac assist pumps. Despite their excellent biocompatibility, these materials may, in certain cases, promote increased blood coagulation [57]. A potential strategy to mitigate this limitation involves surface modification. One approach, introduced in the 1980s, involved powder sintering on blood-contacting surfaces to promote endothelialization; however, the outcomes reported in subsequent decades have been highly variable and difficult to predict [57].

According to the literature, increased surface roughness may enhance biocompatibility by promoting cell adhesion and supporting cellular proliferation [15]. This concept has been implemented in the HeartMate LVAD family, where textured surfaces were designed to facilitate biological integration [57]. Another surface modification strategy, classified as a biological approach, involves coating pump components with heparin to reduce the risk of coagulation [15]. Heparin is a well-established anticoagulant widely used during surgical procedures to prevent clot formation [58].

Polymers constitute another important class of materials used in blood pump components. Polyethylene terephthalate (PET) and polytetrafluoroethylene (PTFE) are commonly employed in the fabrication of cannulas, with polyurethanes being used for pump housing construction as well as elastomeric structural components [59]. Their widespread use is primarily attributed to their flexibility and mechanical strength, which are essential for long-term operation under physiological conditions.

Numerical Simulations (FVM)

Recent research on modeling centrifugal blood pumps demonstrates substantial progress in areas such as computational fluid dynamics (CFD – Computational Fluid Dynamics), turbulence modeling, hemolysis prediction, and geometric optimization. Modern simulations typically employ incompressible Navier–Stokes equations, which describe the motion of viscous fluids, together with turbulence models from the RANS family (Reynolds-Averaged Navier–Stokes). Among these, the SST k–ω model (Shear Stress Transport k–omega) is widely used because it provides improved accuracy in near-wall regions compared with traditional k–ε models [60].

In recent years, high-fidelity modeling strategies have become increasingly common. Approaches such as LES (Large Eddy Simulation) and hybrid methods like SBES

TABLE 2. Major material classes used in cardiac assist devices and their key properties

Material class	Key roles in cardiac assist systems	Key strengths	Key limitations	References
Metals (Ti, SS, Co–Cr–Mo)	Mechanical heart valves, LVAD housings, stents, pacemaker leads	High strength, processable via AM, forging, machining	Ion release, corrosion, limited hemocompatibility	[44, 45]
Polyurethanes (PU, PEU, PCU)	Blood sacs, polymer valves	Flex fatigue resistance, elasticity, tunable structure	Long-term biodegradation, stress cracking, calcification	[46, 47, 48]
Biodegradable polymers (PCL, PLA, PHAs)	Cardiac patches, vascular grafts, engineered valves	Biocompatibility, processable, shape control	Mechanical strength limits, immune response variability	[49, 50, 51]
Composite/ nanocomposites	Conductive scaffolds, patch reinforcement	Enhanced electrical, mechanical behavior	Complexity, long-term behavior uncertain	[52, 53]
Natural biomaterials (collagen, fibrin, alginate, silk)	Cardiac patches, engineered myocardium	High biocompatibility	Low mechanical strength, maturation challenges	[51]
Carbon-based coatings (DLC, a-C:H)	Mechanical valves, VAD components	Improved hemocompatibility, low friction	Microcracks, potential thrombogenicity in long-term	[54, 55]
Soft elastomers (silicone, hot-vulcanized rubber)	Valves	Biomimetic deformation, reduced thrombosis	Durability constraints	[56]

(Stress-Blended Eddy Simulation) allow researchers to capture unsteady, three-dimensional flow structures and to more accurately predict shear-related blood damage. However, these methods require significantly greater computational resources, which limits their routine use in design optimization workflows [60].

Modeling of blood damage in rotary blood pumps is still largely based on empirical hemolysis models, although complementary tensor-based stress metrics are increasingly used to provide alternative estimates of red blood cell trauma [61]. Recent studies have begun to narrow the gap between computational fluid dynamics and actual biological responses by linking simulated shear-stress environments to platelet activation and subsequent functional impairments. These findings demonstrate that CFD can be a meaningful tool for predicting platelet injury in mechanically assisted circulation, such as ventricular assist devices [62].

At the same time, the field emphasizes the importance of standardized validation procedures. This includes the use of U. S. Food and Drug Administration (FDA) reference geometries—benchmark pump and nozzle models developed by the FDA - as well as multi-laboratory comparison studies. Such inter-laboratory efforts have revealed that numerical results may vary significantly depending on the computational setup, mesh strategy, and solver implementation, underscoring the need for harmonized validation frameworks [63, 64].

Geometric design parameters have a strong impact on the hemocompatibility of rotary blood pumps. Numerical investigations show that increasing the impeller radial gap—the clearance between the rotating impeller and the stationary pump housing—reduces local shear stresses and consequently lowers hemolysis, leading to improved overall pump performance [65]. Similarly, studies of hydrodynamic bearings indicate that enlarging the bearing gap decreases the hemolytic load in pumps equipped with semi-open impellers, where part of the impeller surface is exposed to the flow [66].

Further improvements in blood compatibility are achieved through designs that use magnetic levitation (MagLev). In these systems, the impeller is suspended and driven by magnetic fields, eliminating mechanical contact and minimizing shear exposure. This approach has been successfully demonstrated in prototype cone-shaped MagLev pumps, which show reduced blood trauma compared with mechanically supported designs [67]. Advanced pump-design methodologies increasingly integrate computational fluid dynamics with multi-objective optimization frameworks. Approaches that combine genetic algorithms (GAs) with neural-network-based surrogate models enable simultaneous refinement of both impeller and housing geometry, improving hydraulic efficiency while reducing hemolysis [68]. Heuristic optimization strategies, such as the Bees Algorithm (BA), have also been shown to produce beneficial modifications to impeller side-wall clearances. These adjustments reduce wall-induced shear stresses and enhance overall pump performance [69].

Experimental investigations further confirm the clinical importance of minimizing shear-induced blood damage across different modes of circulatory support, demonstrating that design-driven reductions in shear exposure translate into measurable improvements in blood compatibility [70]. A rapidly expanding research direction in blood-pump

modeling involves uncertainty quantification (UQ – Uncertainty Quantification). Stochastic simulations of the FDA benchmark pump—a standardized reference geometry developed by the U.S. Food and Drug Administration—show that predicted shear stresses and hemolysis levels are highly sensitive to modeling assumptions, including parameter choices and boundary-condition definitions [71].

Further developments in probabilistic CFD demonstrate that pump performance can vary substantially under uncertain operating or physiological conditions [72]. In addition, polynomial chaos expansions (PCE) provide an efficient mathematical framework for propagating uncertainty through hemolysis and blood-damage models, reducing computational cost while maintaining predictive accuracy [73]. Recent experimental studies highlight that biological variability, particularly inter-donor differences in erythrocyte (red blood cell) fragility, has a significant impact on measured hemolysis. These findings underscore the importance of incorporating UQ into modeling workflows to ensure reliable and clinically meaningful predictions [74].

In summary, contemporary research demonstrates substantial advances in CFD-based analysis of centrifugal blood pumps, including improved turbulence modeling, integration of optimization algorithms, and expanded uncertainty assessment. Nevertheless, important challenges remain—most notably the limited ability of current models to capture complex biological mechanisms such as platelet activation, as well as the ongoing need for standardized validation procedures. Addressing these gaps represents a promising path toward the development of safer and more efficient rotary blood-contacting devices.

Materials and Methods

FVM 3D Model of the 2-Degree Blood Rotor

The purpose of these simulations was to evaluate the distributions of pressure, blood velocity, wall shear stresses, and power values (derived from the momentum diagram and corresponding calculations) for the selected Casson blood model [75, 76] and the chosen k-ω SST turbulence model [77, 78] applied to the 2-degree blood rotor. The finite-volume polyhedral mesh was developed with the following parameters: 941 277 cells, 4 341 022 nodes, maximum skewness – 0.4685, maximum aspect ratio – 6.31 and minimum orthogonal quality – 0.2856. The last three values represent the worst-case mesh quality parameters, occurring in only a few cells of the finite volume method (FVM) mesh, primarily in non-critical regions of the computational domain. Overall, the average mesh quality is very high, ensuring reliable and accurate simulations. The computational mesh was selected after performing a mesh convergence analysis, leading to the choice of a mesh with six inflation layers for enhanced accuracy. FIG. 2 illustrates the developed FVM mesh of the computational domain, highlighting its main components.

Atmospheric pressure was applied at both the inlet and outlet of the upper and lower sections of the simulated system. The rotor operated at a speed of 5000 rpm, utilizing the k-ω SST turbulence model. Morphological parameter values influence blood density; however, in most cases, it is assumed to be a constant value of 1060 kg·m^{-3} [79-81]. This simplification is valid in simulations of healthy individuals, as significant variations in blood density typically occur only in cases of pathological conditions. A stationary wall with no-slip shear conditions was applied to the fluid domains represented by the cylinder. The solution methods chosen for the simulation included: pressure-velocity coupling with a coupled spatial discretization scheme and transient formulation using second-order implicit scheme, gradient least-square cell-based method, second-order pressure scheme and second-order upwind momentum scheme. The simulation was divided into 100 000-time steps, employing an adaptive time-stepping method due to the requirement for very small time-step sizes at the initial simulation stages. Computations were performed on a PC equipped with an Intel® Core™ i7-3770 CPU (3.40 GHz) and 32 GB of RAM.

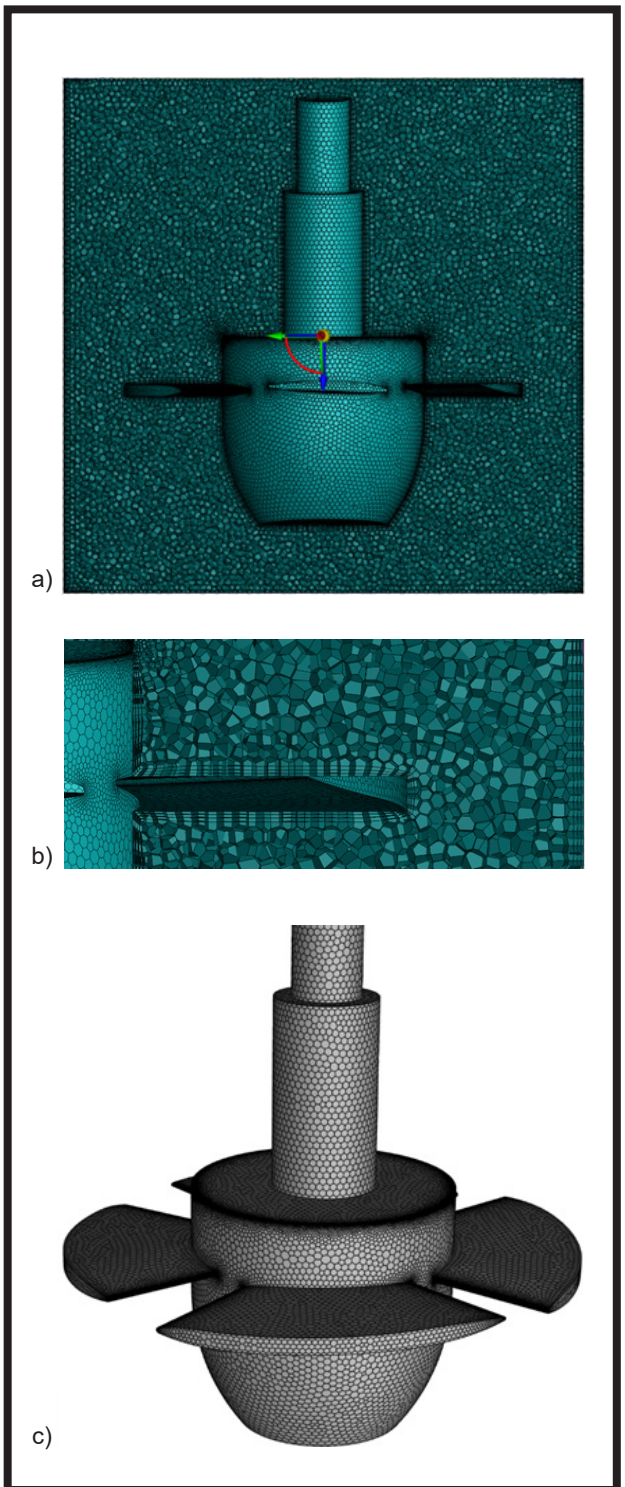

FIG. 2. (a) FVM mesh of the computational domain, (b) enlarged view of the six-layer cell structure near the cylinder walls and rotor blades, and (c) FVM mesh of the rotor

Results and Discussions

Results of FVM 3D Model of the 2-Degree Blood Rotor

The results shown in FIG. 3 illustrate the distributions of contour pressure, wall shear stress vectors, velocity contours, and velocity streamlines. The maximum values of pressure (1,050 kPa), wall shear stress (49.6 kPa), and velocity (98.3 m/s) occurred at the leading edges of the rotor blades. These peaks were confined to small regions of strong flow deceleration and do not represent the overall operating conditions within the pump. The spatially averaged shear stress in the rotor region was 210 Pa, which aligns with reported values for micro-scale rotary pumps (150–500 Pa, with local peaks up to 700–900 Pa) [82-84]. A comparable pattern of moderate bulk shear stresses and confined high-shear regions has been reported for the FDA benchmark blood pump, indicating that such localized maxima are characteristic of rotary pump flow fields rather than deviations from expected performance.

The maximum pressure corresponds to a localized stagnation zone, while the global pressure rise across the device remains low and consistent with micro-pump data at 5000 rpm [85]. A similar distinction between localized blade-surface peaks and global pressure rise is also observed in the FDA benchmark blood pump, where stagnation-zone pressures substantially exceed the device-level pressure head.

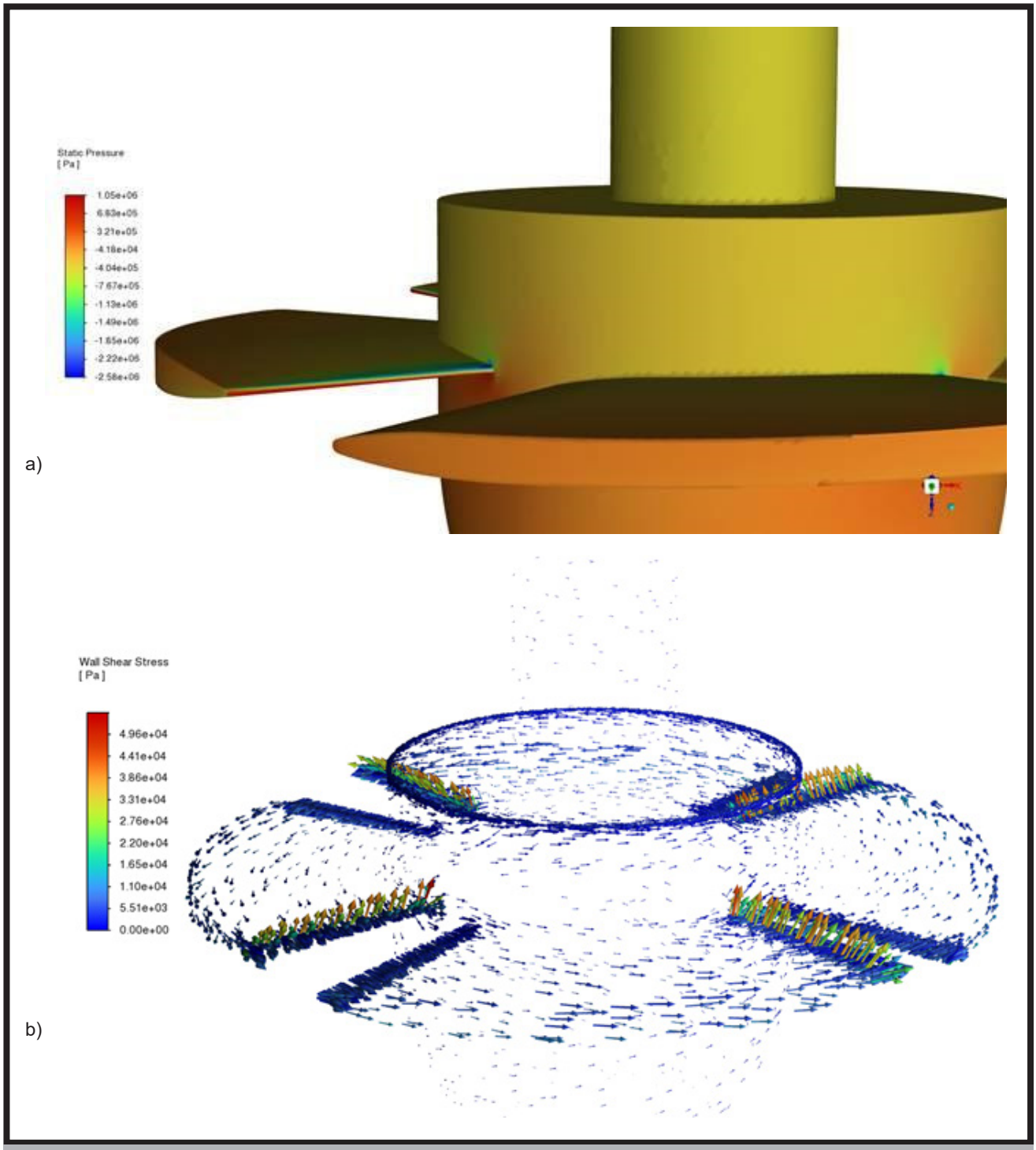

FIG. 3. Distributions of a) pressure contour on the rotor blades, b) shear stress vectors on the rotor blades

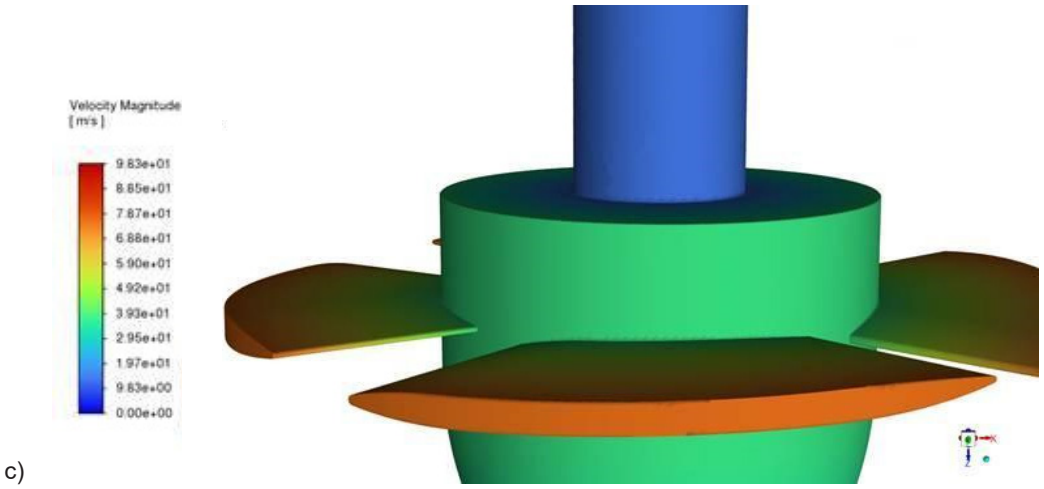

c)

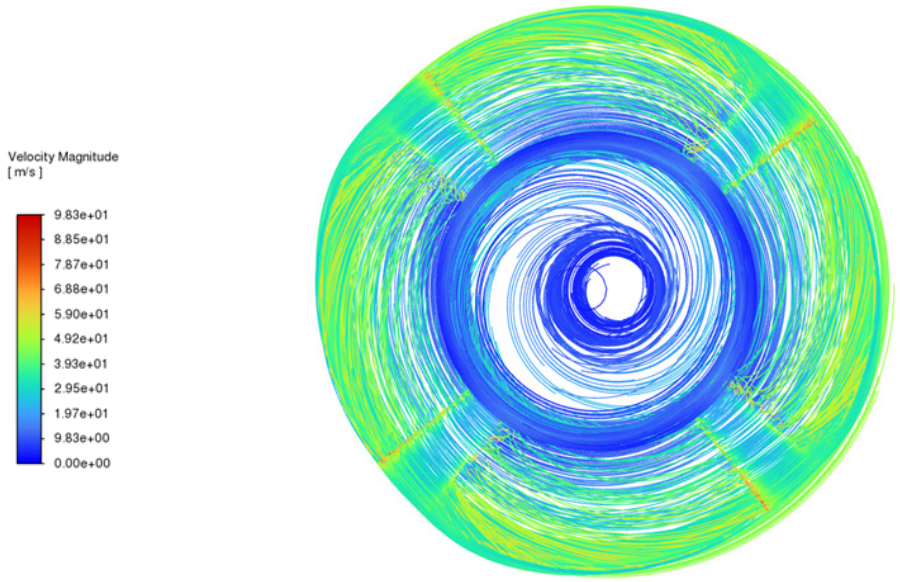

d)

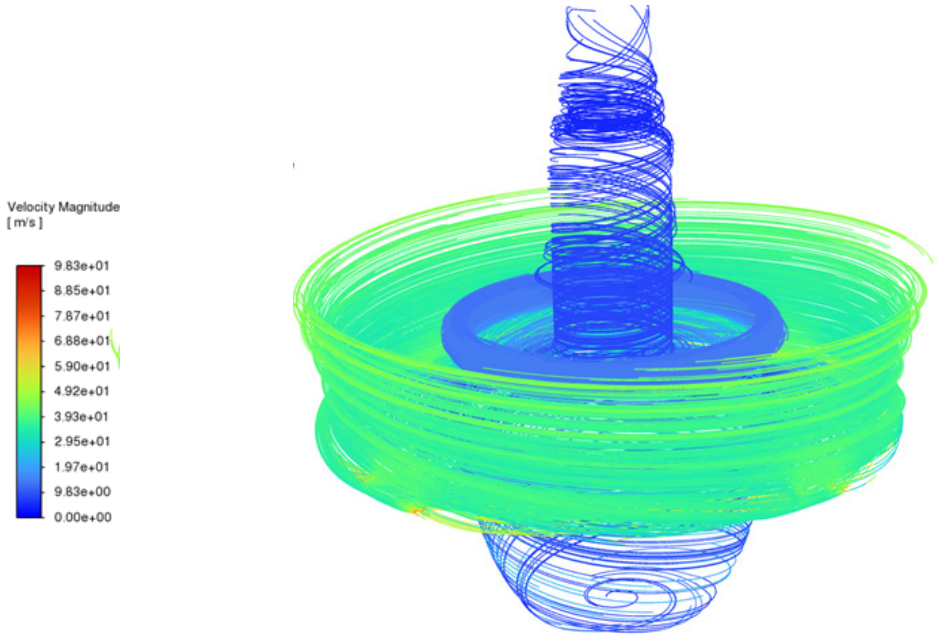

e)

FIG. 3. Distributions of c) velocity contour on the rotor blades, d) velocity streamlines at the bottom of the rotor blades, and e) velocity streamlines (side view)

Using the computed torque of 0.1461 mNm, the hydrodynamic rotor power was 0.0765 W. This value reflects only the mechanical power transferred to the fluid and falls within the expected range for miniature rotary pumps, whose mechanical power typically lies between 0.2 and 0.6 W and whose hydraulic output remains very low (0.01–0.03 W) [84-86]. The magnitude and distribution of mechanical power are consistent with the loss-dominated power balance reported for small-scale pumps and with CFD analyses of the FDA benchmark device. Furthermore, the 2-degree blood rotor generates a vortex that forms around and above the blade surfaces, continuously circulating around the rotor.

Discussion of FVM 3D Model of the 2-Degree Blood Rotor

The results presented in FIG. 3 are consistent with findings in the literature [82-88] on computational fluid dynamics (CFD) simulations of high-speed blood rotor pumps. The regions of highest pressure, velocity, and wall shear stress were located near the blade edges, where the flow undergoes rapid acceleration followed by abrupt deceleration. Such localized extremes are characteristic of high-speed rotary blood pumps and arise from strong shear layers and small-scale turbulent structures forming around the leading edges. The peak wall shear stress of 49.6 kPa reflects these confined conditions and does not represent the shear environment experienced by the bulk flow. Experimental measurements in micro-scale pumps typically show shear stresses of 150–500 Pa, with occasional localized peaks reaching 700–900 Pa [82-84], whereas CFD studies of high-speed impellers demonstrate that blade-surface maxima may exceed these values by more than an order of magnitude [86, 88]. The spatially averaged shear stress of 210 Pa obtained in this study is therefore consistent with both physiological limits and device-scale observations.

A qualitative comparison with the FDA benchmark blood pump further supports the plausibility of the obtained values [89, 90]. The FDA pump exhibits bulk shear stresses of a few hundred pascals and localized wall-shear peaks in the kilopascal range near the cutwater and blade–housing interaction zones. The model shown in the present paper reproduces the same pattern: a physiologically relevant spatially averaged shear stress (210 Pa) and a confined high-shear region at the blade leading edge. The magnitude of the localized peak is therefore consistent with established CFD benchmarks for rotary blood pumps. Although the absolute values differ due to the much smaller geometric scale and higher rotational speed of the present micro-pump model, the underlying flow mechanisms producing localized peaks are the same as those observed in the FDA benchmark device.

The maximum pressure of 1,050 kPa similarly corresponds to a confined stagnation region. In contrast, the overall pressure rise across the pump remains low, matching the characteristic performance of miniature rotary devices, which typically generate 5–30 kPa and approximately 10 kPa at 5000 rpm [84, 85]. This behavior is also consistent with the FDA benchmark pump, where stagnation-zone pressures substantially exceed the global pressure head. This distinction between localized and global pressure behavior is well documented in both experimental and computational analyses of small-scale blood pumps.

The hydrodynamic rotor power of 0.0765 W represents only the mechanical energy imparted to the fluid. Miniature rotary pumps are known to operate with low hydraulic efficiency, as most of the mechanical power is dissipated through viscous shear in narrow gaps, recirculation zones, tip-clearance leakage, and bearing losses. Reported mechanical power levels for devices of similar size and speed are on the order of 0.5 W, while their hydraulic output remains even two orders of magnitude lower (0.01–0.03 W) [85, 86]. The agreement between the simulated power and literature data, together with the qualitative consistency with the FDA benchmark pump, supports the physical realism of the model and confirms that the corrected torque value yields a credible estimate of rotor power for a micro-scale pump operating at 5000 rpm.

The observed velocity (98.3 $m \cdot s^{-1}$) and vortex formation around the rotor blades are well-supported by research on blood flow dynamics. Vortex formation is a common phenomenon in high-speed rotors, contributing to efficient fluid mixing and flow stabilization.

Conclusions and Future Perspectives

Cardiac assist devices, including pulsatile, centrifugal, and axial flow pumps, differ in their operating principles; however, all designs face common challenges related to hemocompatibility, flow-induced stresses, and material performance. Hemocompatibility remains the central challenge in the development of rotary blood pumps and is determined by the combined effects of biomaterial properties and flow conditions within the device. The FVM-based 3D rotor model confirms that the highest values of pressure, velocity, and shear stress occur near blade edges, where flow acceleration and turbulence intensify. These regions represent the most critical zones for hemolysis and platelet activation.

Although titanium alloys and advanced ceramics remain the primary structural materials for blood pump components due to their favorable mechanical properties, their surfaces often require modification to improve blood compatibility. The numerical results demonstrate that even with optimized rotor geometry, localized shear stress hotspots persist, highlighting the importance of surface engineering strategies that minimize adverse blood–material interactions. Among currently investigated surface modification approaches, MPC-based coatings, diamond-like carbon (DLC), and zwitterionic materials demonstrate particularly promising antithrombotic properties. In the context of the identified high-shear regions within the rotor, such coatings may significantly reduce platelet activation and thrombus formation associated with high-speed blood flow.

The performed CFD analysis also confirms that the geometry of rotor blades, clearances, and bearing regions strongly influences pump performance and hemolysis risk. Increasing rotor speed results in higher torque and power values, while vortical flow structures generated around the blades contribute to flow mixing and stabilization. These findings support the need for integrated design strategies combining computational fluid dynamics, experimental validation, and multiparametric optimization. Bearing technology represents another key factor affecting device performance. Magnetic levitation systems, characteristic of third-generation blood pumps, eliminate mechanical contact and therefore reduce friction, heat generation, and additional shear stress within the device.

Future developments in blood pump design may increasingly rely on biomimetic approaches, including endothelialization and biologically inspired surface chemistries. When combined with optimized flow geometries that promote stable, low-shear hemodynamic conditions, such strategies may significantly improve the hemocompatibility of blood-contacting devices and reduce the reliance on synthetic antithrombotic coatings.

Acknowledgments

This work was supported by the Österreichische Forschungsförderungsgesellschaft m.b.H. project no. FO999911698.

Part of this work, covering the review of device design, biomaterials, and hemocompatibility complications, was carried out within the project provided by the National Centre for Research and Development project no. LIDER14/0239/2023.

This work was supported by the Polish National Center for Research and Development project no. M-ERA.NET3/2023/98/KIDmicroBLOODpump/2024.

Part of the research was supported by the statutory activities under 16.16.110.663 of AGH University of Krakow. We gratefully acknowledge Polish high performance computing infrastructure PLGrid (HPC Center: ACK Cyfronet AGH) for providing computer facilities and support within computational grant no. PLG/2026/019728.

Author contribution

Zuzanna Zając (A, B, D, E) – 16%; Magdalena Kopernik (A, B, C, D, E, F) – 16%; Justyna Więcek-Chmielarz (B, D) – 8%; Karolina Szawiracz (B, D) – 8%; Przemysław Kurtyka (B, D) – 7%; Marcin Surmiak (A) – 13%; Mirjam Spuller (A) – 6%; Jürgen M. Lackner (A, F) – 13%; Roman Major (A, B, D, F) – 13%; where: A – research concept and design, B – collection and/or assembly of data, C – data analysis and interpretation, D – writing the article, E – critical revision of the article, F – final approval of the article. However, the corresponding author will chiefly be held responsible.

References

[1] *OECD: The State of Cardiovascular Health in the European Union*, OECD Publishing, Paris, 2025. https://doi.org/10.1787/ea7a15f4-en.

[2] Timmis A., Vardas P., Townsend N., Torbica A., Katus H., De Smedt D., Gale C.P., Maggioni A.P., Petersen S.E., Huculeci R., Kazakiewicz D., de Benito Rubio V., Ignatiuk B., Raisi-Estabragh Z., Pawlak A., Karagiannidis E., Treskes R., Gaita D., Beltrame J.F., McConnachie A., Bardinet I., Graham I., Flather M., Elliot P., Mossialos E.A., Weidinger F., Achenbach S., Spaccarotella S.: European Society of Cardiology: cardiovascular disease statistics 2021. *European Heart Journal* 43 (2022) 716–799. doi: 10.1093/eurheartj/ehab892.

[3] *WHO: Cardiovascular diseases* (CVDs), 2025. https://www.who.int/news-room/fact-sheets/detail/cardiovascular-diseases-(cvds).

[4] Masoudkabir F., Mohammadifard N., Mani A., Ignaszewski A., Davis M.K., Vaseghi G., Mansourian M., Franco C., Gotay C., Sarrafzadegan N.: Shared Lifestyle-Related Risk Factors of Cardiovascular Disease and Cancer: Evidence for Joint Prevention. *ScientificWorldJournal 2023* (2023) 1-15. doi: 10.1155/2023/2404806.

[5] Yusuf S., Hawken S., Ounpuu S., Dans T., Avezum A., Lanas F., McQueen M., Budaj A., Pais P., Varigos J., Lisheng L.: Effect of potentially modifiable risk factors associated with myocardial infarction in 52 countries (the INTERHEART study): case-control study. *The Lancet* (2004) 364 937-952. doi: 10.1016/S0140-6736(04)17018-9.

[6] Alahmar L.A.: Dietary fiber influence on overall health, with an emphasis on CVD, diabetes, obesity, colon cancer, and inflammation. *Front. Nutr.* 11 (2024). doi: 10.3389/fnut.2024.1510564.

[7] Mozaffarian D., Appel L.J., Van Horn L.: Components of a cardioprotective diet: new insights. *Circulation* 123 (2011) 2870-2891. doi: 10.1161/CIRCULATIONAHA.110.968735.

[8] Bounader K., Flecher E.: End-stage heart failure: The future of heart transplant and artificial heart. *La Presse Médicale* 53 (2024). doi: 10.1016/j.lpm.2023.104191.

[9] Isath A., Vukićević M., Moayedifar R., Zuckermann A., Mehra, M.R.: Evolving paradigms and future frontiers in heart transplantation in the modern era: a state-of-art focus review. *Journal of Cardiac Failure* (2025). doi: 10.1016/j.cardfail.2025.07.016.

[10] Lund L.H., Khush K.K., Cherikh W.S., Goldfarb S., Kucheryavaya A.Y., Levvey, B.J., Meiser B., Rossano J.W., Chambers D.C., Yusen R.D., Stehlik J.: The Registry of the International Society for Heart and Lung Transplantation: thirty-fourth adult heart transplantation report—2017; focus theme: allograft ischemic time. *The Journal of Heart and Lung Transplantation* 36 (2017) 1037-1046. doi: 10.1016/j.healun.2017.07.019.

[11] Slaughter M.S., Rogers J.G., Milano C.A., Russell S.D., Conte J.V., Feldman D., Sun B., Tatooles A.J., Delgado R.M. 3rd, Long J.W., Wozniak T.C., Ghumman W., Farrar D., Frazier O.H.: Advanced heart failure treated with continuous-flow left ventricular assist device. *New England Journal of Medicine* 361 (2009) 2241-2251. doi: 10.1056/NEJMoa0909938.

[12] Giridharan G.A., Lee T.J., Ising M., Sobieski M.A., Koenig S.C., Gray L.A., Slaughter, M.S.: Miniaturization of mechanical circulatory support systems. *Artificial organs* 36 (2012) 731–739. doi: 10.1111/j.1525-1594.2012.01523.x.

[13] Mohite P.N., Sabashnikov A., Raj B., Hards R., Edwards G., García-Sáez D., Zych B., Husain M., Jothidasan A., Fatullayev J., Zeriouh M., Weymann A., Popov A.F., De Robertis F., Simon A.R.: Minimally Invasive Left Ventricular Assist Device Implantation: A Comparative Study. *Artificial organs* 42 (2018) 1125–1131. doi: 10.1111/aor.13269.

[14] Bluestein D., Chandran K.B., Manning, K.B.: Towards non-thrombogenic performance of blood recirculating devices. *Annals of biomedical engineering* 38 (2010) 1236–1256. doi: 10.1007/s10439-010-9905-9.

[15] Kozakov K., Provaznik Z., Schmid C., Camboni D.: Advancing LVAD Technology: Overcoming Challenges and Shaping the Future of Mechanical Circulatory Support. *J. Clin. Med*. 13 (2024). doi: 10.3390/jcm13247813.

[16] Hosseinipour M., Gupta R., Bonnell M., Elahinia M.: Rotary mechanical circulatory support systems. *Journal of Rehabilitation and Assistive Technologies Engineering* 4 (2017). doi: 10.1177/2055668317725994.

[17] Moctezuma-Ramirez A., Mohammed H., Hughes A., Elgalad A.: Recent developments in ventricular assist device therapy. *Reviews in Cardiovascular Medicine* 26 (2025). doi: 10.31083/RCM25440.

[18] Yazdanpanah-Ardakani K., Niroomand-Oscuii H., Sahebi-Kuzeh Kanan R., Shokri N.: Optimization of a centrifugal blood pump designed using an industrial method through experimental and numerical study. *Scientific Reports* 14 (2024). doi: 10.1038/s41598-024-57019-9.

[19] Fagot J., Bouisset F., Bonello L., Biendel C., Lhermusier T., Porterie J., Roncalli J., Galinier M., Elbaz M., Lairez O., Delmas C.: (2020). Early evaluation of patients on axial flow pump support for refractory cardiogenic shock is associated with left ventricular recovery. *Journal of Clinical Medicine* 9 2020. doi: 10.3390/jcm9124130.

[20] ABIOMED: Impella 5.0 and LD, https://congreso.sectcv.es/wp-content/uploads/2020/10/HCS-EM00883-EN-rA_Impella-5.0-LD-Brochure_FINAL.pdf.
[21] Abbott: HeartMate 3 LVAD With Full Maglev Flow Technology, https://www.cardiovascular.abbott/us/en/hcp/products/heart-failure/left-ventricular-assist-devices/heartmate-3/about.html.
[22] Johnson&Johnson MedTech: Impella 5.5™ with SmartAssist™ Heart Pump, https://www.heartrecovery.com/en-eu/products-and-services/impella/impella-55-with-smartassist-heart-pump.
[23] Abott: CentriMag Acute Circulatory Support with Full MagLev Flow Technology, https://www.cardiovascular.abbott/us/en/hcp/products/heart-failure/mechanical-circulatory-support/centrimag-acute-circulatory-support-system/about.html#:~:text=The%20CentriMag%20is%20an%20acute%20circulatory%20support,**Wide%20blood%2Dflow%20pathways**%20*%20**Automatic%20rotor%20positioning**.
[24] Adedayo P., Wang S., Kunselman A.R., Ündar A. (2014). Impact of pulsatile flow settings on hemodynamic energy levels using the novel diagonal Medos DP3 pump in a simulated pediatric extracorporeal life support system. *World Journal for Pediatric and Congenital Heart Surgery* 5 (2014) 440-448. doi: 10.1177/2150135114526760.
[25] Medtronic: BPX-80 BIO-Pump Plus, centrifugal Blood Pump, https://www.medtronic.com/se-sv/healthcare-professionals/products/cardiovascular/cardiopulmonary/bpx-80-bio-pump-plus-centrifugal-blood-pump/indications-safety-warnings.html.
[26] Loforte A., Botta L., Boschi S., Gliozzi G., Cavalli G.G., Mariani C., Suarez S.M., Pacini, D.: Durable continuous-flow mechanical circulatory support: *State of the Art. Hearts* 2 (2021) 127-138. doi: 10.3390/hearts2010010.
[27]Bernhardt A.M., Blumer V., Vandenbriele C., Schrage B., Mody K., Pappalardo F., Silvestry S., Anderson M., Abraham J., Gage A., Goldstein D., Grant M., Klipa I., Schloglhofer T., Lim S., Moller J., Panholzer B., Molina E., Reinbendt J., Uriel N., Carnicelli A., Potapov E., Kanwar M.: Clinical management of the Impella 5.5 pump. *The Journal of Heart and Lung Transplantation* 44 (2025) 1688-1702. doi: 10.1016/j.healun.2025.06.008.
[28] Terzi A.: Mechanical circulatory support: 60 years of evolving knowledge. *The International Journal of Artificial Organs* 42 (2019) 215-225. 10.1177/0391398818822267.
[29] Foundation for Cardiac Surgery Development, https://frk.pl/.
[30] Simon M.A., Bachman T.N., Watson J., Baldwin J.T., Wagner W.R., Borovetz H.S.: Current and future considerations in the use of mechanical circulatory support devices: an update, 2008–2018. *Annual Review of Biomedical Engineering* 21 (2019) 33-60. doi: 10.1146/annurev-bioeng-062117-121120.
[31] Kafagy D., Gitano-Briggs H.: Axial Flow Artificial Heart Blood Pumps: A Brief Review. *Trends in Biomaterials & Artificial Organs* 27 (2013) 124-130.
[32] Ahmed A., Wang X., Yang M.: Biocompatible materials of pulsatile and rotary blood pumps: A brief review. *Reviews on Advanced Materials Science* 59 (2020) 322-339. doi: 10.1515/rams-2020-0009.
[33] Curtis J.J., Walls J.T., Wagner-Mann C.C., Schmaltz R.A., Demmy T.L., McKenney C.A., Mann F.A.: Centrifugal pumps: description of devices and surgical techniques. *The Annals of thoracic surgery* 68 (1999) 666-671. doi: 10.1016/s0003-4975(99)00583-4.
[34] Smith P.A., Wang Y., Frazier O.H.: The evolution of durable, implantable axial-flow rotary blood pumps. *Texas Heart Institute Journal* 50 (2023). doi: 10.14503/THIJ-22-7908.
[35] Song X., Throckmorton A L., Untaroiu A., Patel S., Allaire P.E., Wood H.G., Olsen D.B.: Axial flow blood pumps. *ASAIO journal* 49 (2003) 355-364. doi: 10.1097/01.MAT.0000074117.00332.0D.
[36] Hernandez G.A., Nunez Breton J.D., Chaparro S.V.: Driveline infection in ventricular assist devices and its implication in the present era of destination therapy. *Open journal of cardiovascular surgery* 9 (2017). doi: 10.1177/1179065217714216.
[37] Willey J.Z., Gavalas M.V., Trinh P.N., Yuzefpolskaya M., Garan A.R., Levin A.P., Takeda K., Takayama H., Fried J., Naka Y., Topakara V. K., Colombo P.C.: Outcomes after stroke complicating left ventricular assist device. *The Journal of Heart and Lung Transplantation* 35 (2016) 1003-1009. doi: 10.1016/j.healun.2016.03.014.
[38] Federici A.B.: The factor VIII/von Willebrand factor complex: basic and clinical issues. *Haematologica* 88 (2003).
[39] Post A., Wang E., Cosgriff-Hernandez E.: A Review of Integrin-Mediated Endothelial Cell Phenotype in the Design of Cardiovascular Devices. *Ann Biomed Eng* 47 (2019) 366–380. doi: 10.1007/s10439-018-02171-3.
[40] Ul-Islam M., Alabbosh K.F., Manan S., Khan S., Ahmad F., Ullah M.W.:. Chitosan-based nanostructured biomaterials: Synthesis, properties, and biomedical applications. *Advanced Industrial and Engineering Polymer Research* 7 (2024) 79-99. doi: 10.1016/j.aiepr.2023.07.002.
[41] Liu X., Huang C., Sheng Y., Chen Q., Wang Q.: Optimization of hemolytic performance of artificial heart pump based on CFD. *Heliyon*, 11 (2025). doi: 10.1016/j.heliyon.2025.e42635.
[42] Nascimbene A., Bark D., Smadja D.M.: Hemocompatibility and biophysical interface of left ventricular assist devices and total artificial hearts. *Blood* 143 (2024) 661-672. doi: 10.1182/blood.2022018096.
[43] Ratner B.D.: The Biocompatibility Manifesto: Biocompatibility for the Twenty-first Century. *J. of Cardiovasc. Trans. Res.* 4 (2011) 523–527. doi: 10.1007/s12265-011-9287-x
[44] O'Dwyer J., Wylie R., Cryan S.A., Duffy G.P., Dolan E.B.: *Cardiac responses to biomaterials. Handbook of Biomaterials Biocompatibility*, Woodhead Publishing 2020. doi: 10.1016/B978-0-08-102967-1.00025-6.
[45] Munir K., Biesiekierski A., Wen C., Li Y.: *Biodegradable alloys. Structural Biomaterials*, Woodhead Publishing 2021. doi: 10.1016/B978-0-12-818831-6.00001-X.
[46] Phillips R.E., Smith M.C., Thoma, R.J.: Biomedical applications of polyurethanes: implications of failure mechanisms. *Journal of biomaterials applications* 3 (1988) 207-227. doi: 10.1177/088532828800300204
[47] Li W., de Oliveira D.C., Lawless B.M., Lavecchia C.E., Crolla J., Thomas-Seale L.E., Shepherd D.E., Espino D.M.: Dynamics of soft connective tissues and implications for synthetic biomaterials: interfacing the frequency and time domains. *Journal of the Mechanical Behavior of Biomedical Materials* 171 (2025). doi: 10.1016/j.jmbbm.2025.107143.
[48] Miri Z., Farè S., Ma Q., Haugen H.J.: Updates on polyurethane and its multifunctional applications in biomedical engineering. *Progress in Biomedical Engineering* 5 (2023). doi: 10.1088/2516-1091/acef84.
[49] Chang T., Liu C., Lu K., Wu Y., Xu M., Yu Q., Shen Z., Jiang T., Zhang, Y.: Biomaterials based cardiac patches for the treatment of myocardial infarction. Journal of Materials Science & Technology 94 (2021) 77-89. doi: 10.1016/j.jmst.2021.03.062.

[50] Chen Y., Qi Z. D., Ji R., Shi N., Chen H., Wei D.X.: Synthetic biology for scalable production of medical polyhydroxyalkanoates: *Advances and applications. Biotechnology Advances* 86 (2025). doi: 10.1016/j.biotechadv.2025.108722.
[51] Majid Q.A., Fricker A.T., Gregory D.A., Davidenko N., Hernandez Cruz O., Jabbour R.J., Owen T.J., Basnett P., Lukasiewicz B., Stevens M., Best S., Cameron R., Sinha S., Harding S.E., Roy, I.: Natural biomaterials for cardiac tissue engineering: a highly biocompatible solution. *Frontiers in cardiovascular medicine* 7 (2020). doi: 10.3389/fcvm.2020.554597.
[52] Amin D.R., Sink E., Narayan S.P., Abdel-Hafiz M., Mestroni L., Peña B.: Nanomaterials for cardiac tissue engineering. *Molecules* 25 (2020). doi: 10.3390/molecules25215189.
[53] Khan T., Vadivel G., Ayyasamy K., Murugesan G., Sebaey T.A.: Advances in conductive biomaterials for cardiac tissue engineering: design, fabrication, and functional integration. *Polymers* 17 (2025). doi: 10.3390/polym17050620.
[54] Major R., Gawlikowski M., Plutecka H., Surmiak M., Kot M., Dyner M., Lackner J.M., Major B.: Biocompatibility testing of composite biomaterial designed for a new petal valve construction for pulsatile ventricular assist device. *Journal of Materials Science: Materials in Medicine* 32 (2021). doi: 10.1007/s10856-021-06576-w.
[55] Coronel-Meneses D., Sánchez-Trasviña C., Ratera I., Mayolo-Deloisa K.: Strategies for surface coatings of implantable cardiac medical devices. *Frontiers in Bioengineering and Biotechnology* 11 (2023). doi: 10.3389/fbioe.2023.1173260.
[56] Zrinscak D., Lorenzon L., Maselli M., Cianchetti, M.: Soft robotics for physical simulators, artificial organs and implantable assistive devices. *Progress in Biomedical Engineering* 5 (2023). doi: 10.1088/2516-1091/acb57a.
[57] He W., Butcher J.T., Rowlands G.W., Antaki, J.F.: Biological Response to Sintered Titanium in Left Ventricular Assist Devices: Pseudoneointima, Neointima, and Pannus. *ASAIO Journal* 69 (2023) 1–10. doi: 10.1097/MAT.0000000000001777.
[58] Butt S.P., Kakar V., Kumar A., Razzaq N., Saleem Y., Ali B., Raposo N., Ashiq F., Ghori A., Anderson P., Srivatav N., Aljabery Y., Abdulaziz S., Darr U., Bhatnagar, G.: Heparin resistance management during cardiac surgery: a literature review and future directions. *The Journal of ExtraCorporeal Technology* 56 (2024) 136-144. doi: 10.1051/ject/2024015.
[59] Padsalgikar A.D.: *6 – Medical Applications of Polyurethanes In Plastics Design Library, Applications of Polyurethanes in Medical Devices*, William Andrew Publishing 2022. doi: 10.1016/B978-0-12-819673-1.00005-3.
[60] Pan Z., Gao F., Wu P.: Turbulence modelling technique have significant effects on the optimization of centrifugal blood pumps. *IEEE Access* 13 (2025) 95609-95617. doi: 10.1109/ACCESS.2025.3568301.
[61] Arora D., Behr M., Pasquali M.: A tensor-based measure for estimating blood damage. *Artificial organs* 28 (2004) 1002-1015. doi: 10.1111/j.1525-1594.2004.00072.x.
[62] Zhang J., Han D., Chen Z., Wang S., Sun W., Griffith B.P., Wu Z.J.: Linking computational fluid dynamics modeling to device-induced platelet defects in mechanically assisted circulation. *ASAIO Journal*, 70 (2024) 1085-1093. doi: 10.1097/MAT.0000000000002242.
[63] Malinauskas R. A., Hariharan P., Day S. W., Herbertson L. H., Buesen M., Steinseifer U., Aycock K.I., Good B.C., Deutsh S., Manning K.B., Craven, B. A.: *FDA benchmark medical device flow models for CFD validation*. American Society for Artificial Internal Organs (ASAIO) Platinum 70th Anniversary Special Edition, CRC Press 2024.
[64] Ponnaluri S.V., Hariharan P., Herbertson L.H., Manning K.B., Malinauskas R.A., Craven, B.A.: Results of the interlaboratory computational fluid dynamics study of the FDA benchmark blood pump. *Annals of Biomedical Engineering* 51 (2023) 253-269. doi: 10.1007/s10439-022-03105-w.
[65] Lv S., He Z.P., Liu G.M., Hu S.S.: Numerical simulation on the effect of impeller radial gap on hemodynamics and hemocompatibility of a centrifugal blood pump. *Computer Methods in Biomechanics and Biomedical Engineering* (2024) 1-12. doi: 10.1080/10255842.2024.2448299.
[66] Kosaka R., Nishida M., Maruyama O., Yambe T., Imachi K., Yamane T.: Effect of a bearing gap on hemolytic property in a hydrodynamically levitated centrifugal blood pump with a semi-open impeller. *Bio-medical materials and engineering* 23 (2013) 37-47. doi: 10.3233/BME-120730.
[67] Hijikata W., Shinshi T., Shimokohbe A., Sobajima H., Takatani S.: *Disposable MagLev centrifugal blood pump utilizing cone-shaped impeller*. 2008 IEEE/ASME International Conference on Advanced Intelligent Mechatronics (2008) 570-575. doi: 10.1111/j.1525-1594.2009.00957.x.
[68] Ghadimi B., Nejat A., Nourbakhsh S.A., Naderi N.: Multi-objective genetic algorithm assisted by an artificial neural network metamodel for shape optimization of a centrifugal blood pump. *Artificial organs* 43 (2019) E76-E93. doi: 10.1111/aor.13366.
[69] Onder A., Incebay O., Sen M.A., Yapici R., Kalyoncu M.: Heuristic optimization of impeller sidewall gapsbased on the bees algorithm for a centrifugal blood pump by CFD. *The International Journal of Artificial Organs*, 44 (2021) 765-772. doi: 10.1177/03913988211023773.
[70] Li Y., Liu X., Sun A., Deng X., Chen Z., Fan Y.: Multi-method investigation of blood damage induced by blood pumps in different clinical support modes. *ASAIO Journal* 70 (2024) 280-292. doi: 10.1097/MAT.0000000000002116.
[71] Karimi M.S., Razzaghi P., Raisee M., Hendrick P., Nourbakhsh A.: Stochastic simulation of the FDA centrifugal blood pump benchmark. *Biomechanics and Modeling in Mechanobiology*, 20 (2021) 1871-1887. doi: 10.1007/s10237-021-01482-0.
[72] Mohammadi R., Karimi M.S., Raisee M., Sharbatdar M.: Probabilistic CFD analysis on the flow field and performance of the FDA centrifugal blood pump. *Applied Mathematical Modelling* 109 (2022) 555-577.
[73] Schick M., Song C., Heuveline, V.: *A polynomial chaos method for uncertainty quantification in blood pump simulation*. Proceedings of the 1st ECCOMAS Thematic Conference on Uncertainty Quantification in Computational Sciences and Engineering (UNCECOMP 2015), Crete Island, Greece (2015).
[74] Blum C., Mous M., Steinseifer U., Clauser J.C., Neidlin M.: Quantifying Experimental Variability in Shear-Induced Hemolysis to Support Uncertainty-Aware Hemolysis Models: C. Blum et al. *Annals of Biomedical Engineering* 53 (2025) 2551-2561. doi: 10.1007/s10439-025-03786-z.
[75] Wajihah S.A., Sankar, D.S.: A review on non-Newtonian fluid models for multi-layered blood rheology in constricted arteries. *Archive of Applied Mechanics* 93 (2023) 1771-1796. doi: 10.1007/s00419-023-02368-6.

[76] Szeliga D., Kopernik M., Pietrzyk M.: Critical evaluation and sensitivity analysis of rheological models of human blood. *Computer Methods in Materials Science* 9 (2009) 435-450.
[77] Menter F. R.: Two-equation eddy-viscosity turbulence models for engineering applications. *AIAA Journal* 32 (1994) 1598-1605.
[78] Kopernik M., Dyrda K., Kurtyka P., Major R.: Discrete phase model of blood flow in a roughness microchannel simulating the formation of pseudointima. *Acta of Bioengineering and Biomechanics*, 24 (2022) 131-144. doi: 10.37190/ABB-01989-2021-02.
[79] Kozłowski M., Wojtas K., Orciuch W., Smolka G., Wojakowski W., Makowski Ł.: Parameters of flow through paravalvular leak channels from computational fluid dynamics simulations—data from real-life cases and comparison with a simplified model. *Journal of Clinical Medicine* 11 (2022). doi: 10.3390/jcm11185355.
[80] Wojtas K., Kozłowski M., Orciuch W., Makowski Ł.: Computational fluid dynamics simulations of mitral paravalvular leaks in human heart. *Materials* 14 (2021). doi: 10.3390/ma14237354.
[81] Krystian J., Łukasz M., Wojciech O.: Model of blood rheology including hemolysis based on population balance. *Communications in Nonlinear Science and Numerical Simulation* 116 (2023). doi: 10.1016/j.cnsns.2022.106802.
[82] Mizunuma H., Nakajima R.: Experimental study on shear stress distributions in a centrifugal blood pump. *Artificial Organs* 31 (2007) 283–289. doi: 10.1111/j.1525-1594.2007.00421.x.
[83] Wang S., Griffith B.P., Wu Z.J.: Device-Induced Hemostatic Disorders in Mechanically Assisted Circulation. *Clinical and Applied Thrombosis/Hemostasis* 27 (2021) 1–14. doi: 10.1177/1076029620982374.
[84] Takatani S., Hoshi H., Tajima K., et al.: Feasibility of a miniature centrifugal rotary blood pump for low-flow circulation in children and infants. *ASAIO Journal* 51 (2005) 563–568. doi: 10.1097/01.mat.0000176139.01152.5b.
[85] Ahn C.H., Allen M.G.: *Fluid micropumps based on rotary magnetic actuators*. Proceedings of the IEEE Micro Electro Mechanical Systems (1995).
[86] Hijikata W., Mamiya T., Shinshi T., Takatani S.: A cost-effective extracorporeal magnetically levitated centrifugal blood pump. Proc. IMechE Part H: *Journal of Engineering in Medicine* 225 (2011) 1051–1060. doi: 10.1177/0954411911422842.
[87] Bartoli C.R., Kang J., Zhang D., et al.: LVAD design reduces von Willebrand factor degradation. *Annals of Thoracic Surgery* 103 (2017) 123–130. doi: 10.1016/j.athoracsur.2016.06.112.
[88] Chua L.P., Su B., Lim T.M., Zhou T.: Numerical simulation of an axial blood pump. *Artificial Organs* 31 (2007) 560–570. doi: 10.1111/j.1525-1594.2007.00422.x.
[89] Ponnaluri S. V., Hariharan P., Herbertson L. H., Craven B. A.: Results of the interlaboratory computational fluid dynamics study of the FDA benchmark blood pump. *Annals of Biomedical Engineering* 51 (2023) 1–15. doi: 10.1007/s10439-022-03105-w.
[90] Good B. C., Manning K. B.: Computational modeling of the Food and Drug Administration's benchmark centrifugal blood pump. *Artificial Organs* 44 (2020) 744–756. doi: 10.1111/aor.13643.